

The effect of pressure upon hydrogen bonding in chlorite: A Raman spectroscopic study of clinochlore to 26.5 GPa

ANNETTE K. KLEPPE,^{1,*} ANDREW P. JEPHCOAT,¹ AND MARK D. WELCH²

¹Department of Earth Sciences University of Oxford, Parks Road, Oxford, OX1 3PR, U.K.

²Department of Mineralogy, The Natural History Museum, Cromwell Road, London SW7 5BD, U.K.

ABSTRACT

The effect of pressure upon hydrogen bonding in synthetic end-member clinochlore, $(\text{Mg}_5\text{Al})(\text{Si}_3\text{Al})\text{O}_{10}(\text{OH})_8$, has been studied in situ by high-pressure micro-Raman spectroscopy in a moissanite-anvil cell to 26.5 GPa at 300 K. The ambient spectrum consists of three OH-stretching bands between 3400 and 3650 cm^{-1} , attributed to the hydrogen-bonded interlayer OH, and a narrow band at 3679 cm^{-1} that is assigned to the non-hydrogen-bonded OH groups of the talc-like 2:1 layer. The pressure dependence of the OH modes is linear up to 6 GPa. Near 9 GPa a major discontinuity occurs in the pressure dependence of the interlayer OH-stretching modes. It involves frequency increases $>100 \text{ cm}^{-1}$ that indicate major changes in hydrogen bonding. The OH mode of the 2:1 layer does not show discontinuous behavior at 9 GPa. A further discontinuity occurs at ~ 16 GPa. This discontinuity affects both interlayer and 2:1 OH, and is likely to be associated with a change in the overall compression mechanism of clinochlore. The spectroscopic behavior is a completely reversible function of pressure. Predictions based upon recent high-pressure diffraction studies of hydrogen bonding and compression of clinochlore suggest that the 9 GPa transition is associated with attainment of an $\text{O}^{2-}\text{-O}^{2-}$ -contact distance of 2.7 Å.

INTRODUCTION

The range of minerals in the Earth capable of hosting water in the form of H_2O and/or OH ranges from ice to nominally anhydrous silicate phases. Chlorite, one of the most OH-rich silicates, is a major constituent of hydrated oceanic crust and may have a significant role as a water carrier in cold, old subduction zones (Peacock 1990). The Mg end-member chlorite, clinochlore $(\text{Mg}_5\text{Al})(\text{Si}_3\text{Al})\text{O}_{10}(\text{OH})_8$, is expected to be the major aluminous phase in low-alkali hydrous peridotites below 800 °C (Jenkins 1981).

The crystal structure of chlorite is characterized by an alternation of a talc-like 2:1 layer (two opposing tetrahedral sheets with an octahedral sheet between them) and a brucite-like layer (Fig. 1). Bonding between these layers involves only hydrogen bonds. In the case of end-member clinochlore, the octahedra of the 2:1 layer are fully occupied by Mg, and those of the brucite-like layer have the following occupancies: M3 = Mg, M4 = Al (M3:M4 = 2:1). Increasing Al substitution in clinochlore via the Mg-Tschermak's exchange, ${}^6\text{Mg} + {}^4\text{Si} \leftrightarrow {}^6\text{Al} + {}^4\text{Al}$, involves only compositional changes in the 2:1 layer; the cation composition of the brucite-like layer remains fixed at Mg_2Al . Brown and Bailey (1962) derived the twelve regular one-layer chlorite polytypes that arise from different ways of stacking the 2:1 and brucite-like layers with stacking vectors defining translations within the plane of the polyhedral sheets and also reversals of the "slant direction" of the octahedral sheets of the two layers (parallel, anti-parallel). The one-layer

monoclinic *I1b-2* (*C2/m*) and triclinic *I1b-4* polytypes (*C $\bar{1}$*) are common in nature. The triclinic *I1b-4* polytype is metrically monoclinic ($\beta \sim 97^\circ$), and only slight differences exist between the X-ray powder diffraction patterns of these two polytypes. Both polytypes have the reversed slant orientation of the octahedra of the 2:1 and brucite-like layers (both are class II polytypes). The main structural difference between *I1b-2* and *I1b-4* polytypes is that in the latter the two tetrahedral sheets are staggered relative to each other, thus breaking mirror and diad symmetry. This offset also results in a different configuration for the OH groups of the 2:1 layer. The consensus of studies on end-member clinochlore synthesized at high-pressure favors, albeit marginally, the *I1b-2* polytype (Jenkins and Chernosky 1986; Bailey 1988; Welch et al. 1995; Baker and Holland 1996). This opinion was confirmed in the neutron diffraction study of synthetic clinochlore by Welch and Marshall (2001). Hereafter, we refer to *I1b-2* as "*C2/m*" and *I1b-4* as "*C $\bar{1}$* ."

The hydrogen bonds of H2 and H3 in synthetic *C2/m* clinochlore are 1.9 and 2.1 Å long (Welch and Marshall 2001), and are of moderate strength. In *C2/m* clinochlore, Al and Si mix statistically at just one tetrahedral site, but there is a high degree of short-range Al-Si order at tetrahedral sites and Al-O-Al avoidance operates (Welch et al. 1995). Such ordering leads to only two different configurations for bridging O atoms, Si-O-Si and Si-O-Al. The NMR study of Welch et al. (1995) did not see any evidence for long-range ordering at two non-equivalent tetrahedral sites.

Our motivation to investigate clinochlore was stimulated

* E-mail: Annette.Kleppe@earth.ox.ac.uk

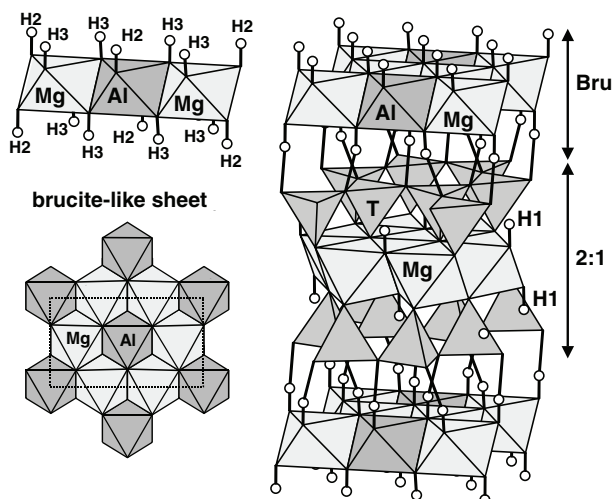


FIGURE 1. The structure of monoclinic $C2/m$ clinocllore (right). Hydrogen bonds link brucite-like (Bru) and 2:1 sheets. The cation array of the brucite-like sheet is shown at bottom left with the a - b plane shown dotted. The proton sites of the brucite-like layer are illustrated top left.

not only by its possible importance in subducting water into the upper mantle, but also by fundamental physical processes involved with the response of hydrogen bonding to pressure. To understand the significance and properties of hydrogen bonding in minerals at deep-Earth conditions, spectroscopic data together with complementary direct structural information from diffraction experiments is required at ambient conditions and high pressures. Recently, the structural behavior (to 5 GPa) and the first equation-of-state (to 8 GPa) of clinocllore were determined with high-pressure powder neutron and synchrotron X-ray diffraction, respectively (Welch and Marshall 2001; Welch and Crichton 2002). However, Raman studies of clinocllore are rare and no high-pressure spectroscopic data exist. Therefore, we studied the effect of pressure upon hydrogen bonding in clinocllore with high-pressure micro-Raman spectroscopy in a moissanite-anvil cell to 26.5 GPa at 300 K. Raman spectroscopy is especially sensitive to possible rearrangements of hydrogen atoms in mineral structures, and the use of moissanite anvils ensured low background fluorescence and negligible anvil interference in the OH-stretching region (Xu and Mao 2000). A comparison of our spectroscopic data with the detailed structural information on hydrogen bonding behavior to 5 GPa from a high-pressure neutron diffraction study (Welch and Marshall 2001) allows interpretation of the changes in the Raman spectra with variations in bond distances and angles.

EXPERIMENTAL METHODS

The sample used in this study was from the same batch as that used by Welch et al. (1995) in their NMR study of clinocllore. Clinocllore was synthesized from a stoichiometric gel in a piston-cylinder apparatus at 1.5 GPa and 690–720 °C using a 0.75 inch diameter NaCl pressure cell. The product was monophasic clinocllore free of stacking disorder. Refine-

ment of X-ray powder diffraction data gave the following cell parameters: $a = 5.320(0)$ Å, $b = 9.215(1)$ Å, $c = 14.393(2)$ Å, $\beta = 97.09^\circ$, and $V = 700.2(1)$ Å³ (Welch et al. 1995).

In the high-pressure Raman experiment, compacted clinocllore powder was mounted in a moissanite-anvil cell together with two ruby chips for pressure calibration. Fluid argon was loaded as a pressure-transmitting medium at 0.2 GPa with a gas-loading technique (Jephcoat et al. 1987). Culets 400 μm in diameter and a stainless steel gasket preindented to 65 μm with a 150 μm hole were used. Raman spectra for both increasing and decreasing pressures were recorded in 135° scattering geometry with a SPEX Triplemate equipped with a back-illuminated, liquid-N₂-cooled CCD detector in the range of 100 to 4000 cm^{-1} . The intrinsic resolution of the spectrometer is 1.5 cm^{-1} and calibrations are accurate to ± 1 cm^{-1} . However, the fitted positions of the 3605 and 3647 cm^{-1} OH bands varied by ± 5 –10 cm^{-1} due to their strong overlap and larger peak widths; the accuracy of the lowest OH-stretching mode was limited by low intensity, large half width, and band overlap to ± 15 cm^{-1} . Raman spectra were excited by the 514.5 nm line of an Ar⁺ laser focused down to a 10 μm spot on the sample. The laser power was low enough to avoid heating the sample. Further, the ruby spectra confirmed quasi-hydrostatic conditions over the whole pressure range of this study up to 26.5 GPa. The frequency of each Raman band was obtained by Voigtian curve fitting.

RESULTS

Raman frequencies at ambient conditions

The observed ambient Raman frequencies of synthetic end-member clinocllore agree well with the previous ambient Raman study of natural Mg-chlorite by Prieto et al. (1991) (Table 1). The Raman spectrum is characterized by several strong modes in the range from 100 to 1100 cm^{-1} and by OH modes between 3470 and 3700 cm^{-1} (Fig. 2). Figure 3 illustrates that the minimum number of symmetric peaks needed to fit the OH-stretching bands is four. The OH-stretching bands between 3470 and 3650 cm^{-1} are attributed to hydrogen-bonded interlayer OH (Serratosa and Viñas 1964; Shirozu 1980; Prieto et al. 1991; Welch et al. 1995). The 3477 cm^{-1} mode results from OH-stretching vibrations of $(\text{Mg}_2\text{Al})\text{O}-\text{H}\cdots\text{O}(\text{SiAl})$ and the 3605 and 3647 cm^{-1} bands are due to OH-stretching vibrations of the $(\text{Mg}_2\text{Al})\text{O}-\text{H}\cdots\text{O}(\text{SiSi})$ hydroxyl groups. The highest-frequency and narrow OH band at 3679 cm^{-1} is assigned to the non-hydrogen-bonded hydroxyls of the talc-like 2:1 layer. Its frequency is identical to the frequency of the talc OH mode. The IR spectrum of the same sample revealed only three OH bands (Welch et al. 1995), but at lower resolution than the present Raman experiment.

Deconvolution of the 3630 cm^{-1} feature into two overlapping peaks suggests at least two Raman-active vibrations contribute to this band rather than the one expected for space group $C2/m$. As the 3477 and 3630 cm^{-1} peaks are both due to structurally similar hydrogen-bonded OH groups, we would also expect corresponding additional components in the 3477 cm^{-1} band, although these are not resolved in the spectrum. To explore this possibility further we collected the ambient Raman

TABLE 1. Ambient Raman frequencies and pressure derivatives of the most intense lattice modes and OH-stretching frequencies of clinochlore; for comparison the Raman frequencies of aluminous clinochlore and of a previous study by Prieto et al. (1991) are given

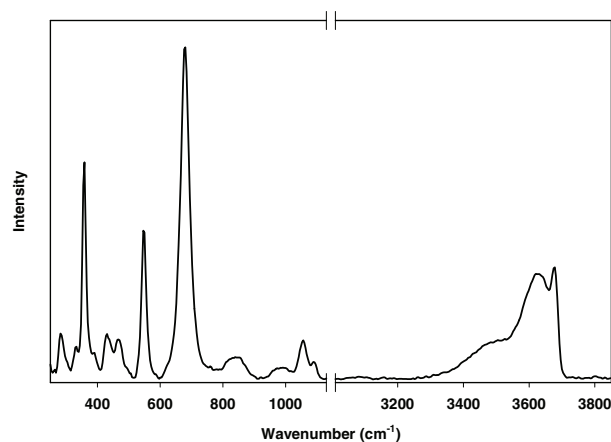
Present study		Prieto et al. (1991), natural Mg-rich chlorite, sample no. P108902	
$(\text{Mg}_5\text{Al})(\text{Si}_2\text{Al})\text{O}_{10}(\text{OH})_8$		$(\text{Mg}_{4.5}\text{Al}_{1.5})(\text{Si}_{2.5}\text{Al}_{1.5})\text{O}_{10}(\text{OH})_8$	
$\nu_i/(\text{cm}^{-1})$	$\left(\frac{\partial \nu_i}{\partial P}\right)_T / \left(\frac{\text{cm}^{-1}}{\text{GPa}}\right)$ to 5.26 GPa	$\nu_j/(\text{cm}^{-1})$	Mode assignment*
104	0.119	105	$\nu_5(\text{F}_{2g}), \text{MO}_6$
198	4.134	197	
358	$2.786P - 0.017P^2$ †	360	$\text{MO}_4(\text{OH})_2, 2:1$
548	$5.255P - 0.109P^2$ †‡	552	$\text{E}_1^2, \nu(\text{T}_2\text{O}_5)$
679	5.475	676	$\text{A}_g^2, \text{E}_g^2, \nu(\text{T}_2\text{O}_5)$
3477	0.011	3455	$\sim 3480 [\perp (001)]$ §
3605	1.679	3541	
3647	0.170	3587	3626 [(001)] 3642 [\perp (001)]
3679	1.545	3641 3675	$\nu_{\text{OH}}, (\text{SiSi})\text{O}\cdots\text{OH}$ $\nu_{\text{OH}}, 2:1$

* Based on a general model of phyllosilicates defined from IR spectra.

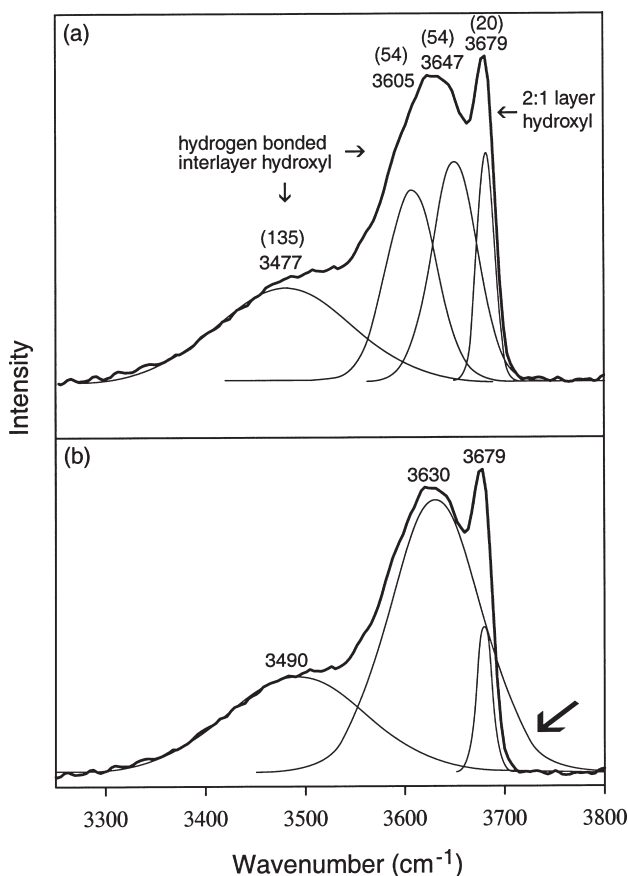
† To 26.5 GPa.

‡ To 14 GPa.

§ Visible in their spectrum.

**FIGURE 2.** Ambient Raman spectrum of clinochlore collected outside the moissanite-anvil cell.

spectrum of a synthetic aluminous clinochlore, $(\text{Mg}_{4.5}\text{Al}_{1.5})(\text{Si}_{2.5}\text{Al}_{1.5})\text{O}_{10}(\text{OH})_8$, also studied by Welch et al. (1995), and related compositionally to end-member clinochlore by 0.5[^6Al $^4\text{Al}^6\text{Mg}_{-1}^4\text{Si}_{-1}$]. As stated above, the composition of the brucite-like layer is not affected by the Mg-Tschermak's exchange, and so the same octahedral configuration surrounds the hydrogen-bonded protons in this chlorite as in end-member clinochlore. Figure 4 shows the OH-stretching modes of aluminous clinochlore. The only significant spectral difference from end-member clinochlore is the presence of a $(\text{Mg}_2\text{Al})\text{O}-\text{H}$ contribution from the 2:1 layer at 3641 cm^{-1} and a corresponding reduced intensity for the $\text{Mg}_3\text{O}-\text{H}$ peak at 3675 cm^{-1} . The latter peak is more clearly separated from the highest-frequency $(\text{Mg}_2\text{Al})\text{O}-\text{H}\cdots\text{O}(\text{SiSi})$ peak in aluminous clinochlore than it is in Mg-rich clinochlore. The association of the 3641 cm^{-1} mode with $(\text{Mg}_2\text{Al})\text{O}-\text{H}$ is supported by its pressure dependence, which is identical to that of the 3675 cm^{-1} 2:1 layer mode, and

**FIGURE 3.** Ambient Raman spectrum of the OH-stretching modes of clinochlore fitted with four (a) and three peaks (b). The FWHM of each peak for the ideal four-peak fit is shown in parentheses above the peak position. The arrow in (b) indicates a clear deficiency of fitting the 3630 cm^{-1} feature with a single peak.

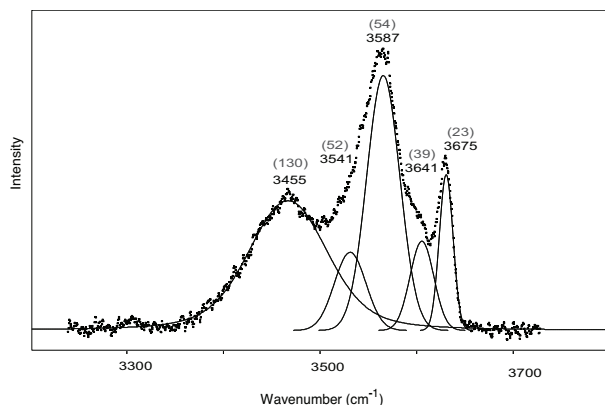


FIGURE 4. OH-stretching modes of aluminous clinochlore. A best fit is obtained with a minimum number of five peaks at ambient conditions. The FWHM of the interlayer OH and 2:1 layer Mg₃O-H mode (shown in parentheses above the peak position) is within error identical to the FWHM of the corresponding modes of end-member clinochlore (Fig. 3).

different from the neighboring 3541 and 3587 cm⁻¹ bands that are associated with (Mg₂Al)O-H...O(SiSi). At 2.5 GPa both the 3641 and 3675 cm⁻¹ mode are only 2 cm⁻¹ higher than at 1 bar, effectively constant within error. On the other hand, the 3541 and 3587 cm⁻¹ bands show clear positive pressure shifts, their peak positions being 13 cm⁻¹ higher at 2.5 GPa than at ambient conditions. The increased intensity of the (Mg₂Al)O-H...O(SiAl) Raman band at 3455 cm⁻¹ in aluminous clinochlore agrees with the increased ⁴Al content. Additional components in this band cannot be resolved, but could be present as is indicated by its large full-width at half-maximum [FWHM is 130 cm⁻¹ compared to 54 cm⁻¹ of the (Mg₂Al)O-H...O(SiSi) bands]. The two-peak nature of the (Mg₂Al)O-H...O(SiSi) hydroxyl vibration in Mg end-member clinochlore is confirmed by a similar doublet structure in the spectra of the aluminous phase. We suggest that the fine structure of the 3630 cm⁻¹ peak reflects a splitting of the corresponding H site in the structure.

Effect of pressure on the Raman frequencies

The use of moissanite anvils in the present high-pressure Raman study of clinochlore ensured low fluorescence and interference-free (e.g., no broad second-order diamond band) Raman spectra in the OH-stretching region. Moissanite has Raman peaks between 100 and 1100 cm⁻¹, which obscure the clinochlore spectra in this range. However, the strongest clinochlore modes did not interfere with the moissanite bands and were tracked reliably to the highest pressure of 26.5 GPa (Figs. 5 and 6, Table 1). All observed modes show positive, linear pressure dependence up to at least 6 GPa with only the 358 cm⁻¹ mode shifting continuously to 26.5 GPa.

The effect of pressure upon hydrogen bonding in clinochlore is considerable. Figure 7 shows the high-pressure evolution of Raman spectra of clinochlore in the OH-stretching region. As for the low-frequency modes (100–1100 cm⁻¹), the pressure dependence of all OH modes is linear up to ~6 GPa (Fig. 8, Table 1). The OH-stretching bands show nearly constant and

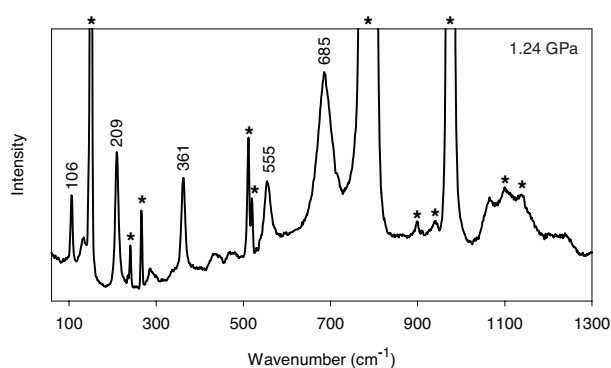


FIGURE 5. Raman spectrum of clinochlore in a moissanite-anvil cell at 1.24 GPa. The peak positions of the most intense clinochlore modes are labeled. The moissanite bands, marked with an asterisk, have been confirmed by measuring the pure moissanite spectrum, away from the sample.

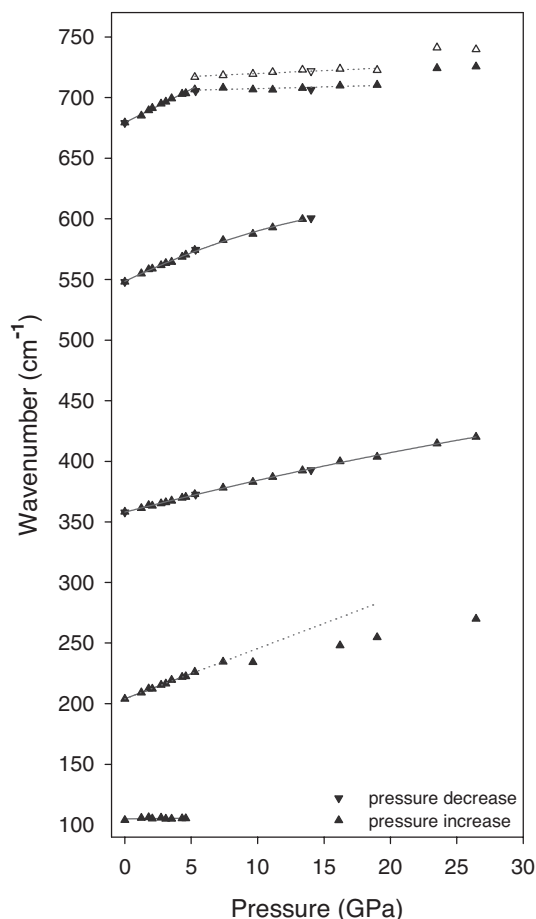


FIGURE 6. Pressure dependence of the lattice Raman modes of clinochlore. The ambient 679 cm⁻¹ mode (closed triangles) shows varying shoulders on its high- and low-frequency side at pressures above 3 GPa, but only one of these shoulders is unambiguously identifiable at more than one pressure point (open triangles). The error in measurement of both frequency and pressure is within the size of the symbol. Solid lines represent the linear or nearly linear pressure dependence of the modes; dotted lines serve as guides for the eye.

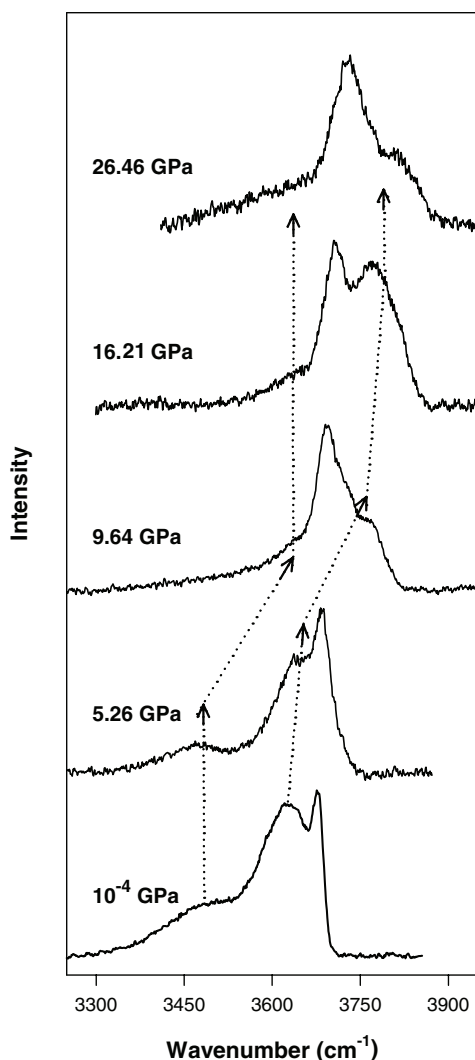


FIGURE 7. Representative Raman spectra of clinochlore as function of increasing pressure in the OH-stretching frequency region. Dotted lines represent schematically the “trajectories” of the OH mode shifts of the $(\text{Mg}_2\text{Al})\text{O}-\text{H}\cdots\text{O}(\text{SiAl})$ and $(\text{Mg}_2\text{Al})\text{O}-\text{H}\cdots\text{O}(\text{SiSi})$ hydroxyl groups.

positive pressure shifts. Near 9 GPa a sharp increase occurs in the frequencies of all hydrogen-bonded interlayer OH modes, manifested as unusually large positive pressure shifts ($\Delta\nu > 100 \text{ cm}^{-1}$). The $(\text{Mg}_2\text{Al})\text{O}-\text{H}\cdots\text{O}(\text{SiAl})$ hydroxyl vibration shifts from 3477 to 3645 cm^{-1} , and the 3605 and 3647 cm^{-1} OH modes shift through the sharper, largely invariant OH-stretching mode of the 2:1 layer to very high frequencies: 3727 and 3768 cm^{-1} at 9.6 GPa. The jump in the pressure dependence is followed by a continued steep increase in their frequencies under further compression, ending in a plateau with frequencies about 3775 and 3820 cm^{-1} at pressures greater than 16 GPa. The discontinuity observed at ~ 16 GPa affects all OH-stretching bands, including the OH mode of the 2:1 layer (3679 cm^{-1}), which had shifted uniformly up to this pressure. Although the pressure dependence of the 3679 cm^{-1} mode is unaffected by the frequency jump of the hydrogen-bonded interlayer OH group at

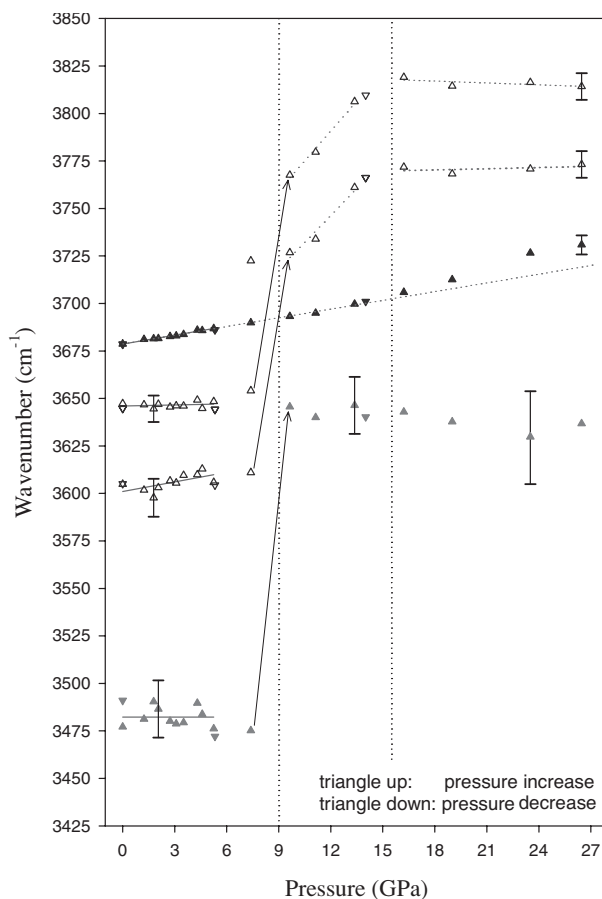


FIGURE 8. Pressure dependence of the OH-stretching modes of clinochlore. Filled grey triangles: interlayer OH mode associated with $(\text{Mg}_2\text{Al})\text{O}-\text{H}\cdots\text{O}(\text{SiAl})$ hydroxyl groups; open triangles: interlayer OH modes associated with $(\text{Mg}_2\text{Al})\text{O}-\text{H}\cdots\text{O}(\text{SiSi})$; closed black triangles: $\text{Mg}_3\text{O}-\text{H}$ mode of the 2:1 layer. Errors in pressure measurement are within the size of the symbol. Errors in frequency are shown by representative error bars; an exception is the ambient 3679 cm^{-1} mode; the error in its frequency is within the size of the symbol to 20 GPa. Solid lines represent the linear pressure dependence of the modes to 5.6 GPa; dotted lines serve as guides to the eye.

~ 9 GPa, this discontinuity appears to be reflected in a pressure-dependent broadening of its FWHM at 9 and again at 16 GPa (Fig. 9). However, this broadening could also indicate the start of H-site disorder. On decompression, all OH-stretching and lattice modes return to their original 1 bar positions without any hysteresis. Changes in both half-widths and intensities of the Raman peaks are reversible. A synchrotron X-ray diffraction study of clinochlore with a helium pressure medium confirmed the Raman transition at 9 GPa (Welch et al., in preparation).

DISCUSSION

Comparison with neutron data to 5 GPa

The response of the OH modes of clinochlore at pressures up to 5 GPa is in overall agreement with the results of the neu-

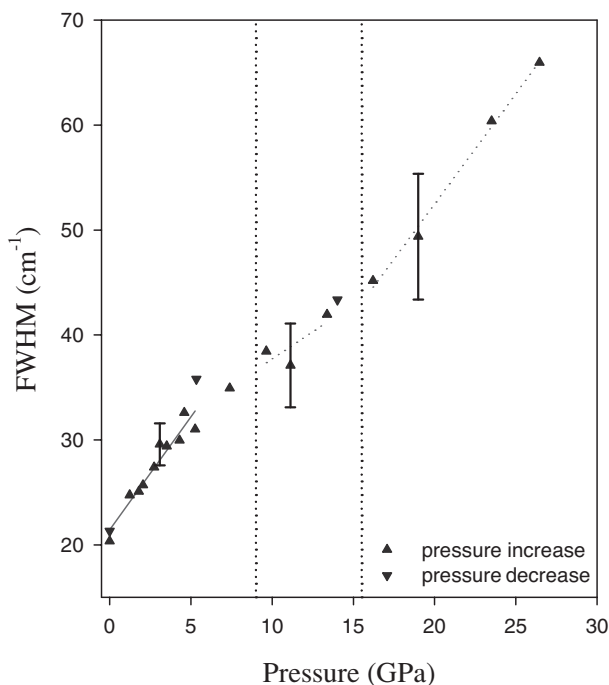


FIGURE 9. Pressure dependence of the FWHM of the OH-stretching mode of the talc-like 2:1 layer (ambient 3679 cm⁻¹).

tron diffraction study of Welch and Marshall (2001). In that study it was observed that the main effect of pressure upon clinocllore is a steady compression of its interlayer achieved by a closing of the O-D...O bond angles (from around 170° at 10⁻⁴ GPa to 150° at 4.7 GPa) with negligible changes in the O-D and D...O bond lengths. The influence of this change in the clinocllore structure under compression on the interlayer OH bands (3477, 3605, and 3647 cm⁻¹) is not obvious. Unusually strong broadening of the modes or significant changes in their intensities do not occur within the limits of determination due to strong peak overlap. Hofmeister et al. (1999) reported that the width of hydrogen-bonded OH modes increases with pressure more for a bent than for a linear bond. However, the role of the hydrogen-bond angle in hydrogen bonding and its detailed influence on the peak parameters of the OH-stretching vibrations needs further study.

The nearly constant and slight positive pressure dependence of the 3647 and 3605 cm⁻¹ OH bands reflects the observed invariant O-D(2) hydroxyl and D(2)...O hydrogen bond lengths (Welch and Marshall 2001). The reported small linear contraction of the D(3)...O hydrogen bond to 4.7 GPa (0.11 Å), possibly with a concomitant lengthening of the O-D(3) bond, is not resolvable within the error of measurement in the Raman data, which shows approximately constant pressure dependencies of all hydrogen-bonded OH groups. The OH mode of the 2:1 layer (3679 cm⁻¹) shifts at a rate of ~1.5 cm⁻¹GPa⁻¹ to higher frequencies under compression. This agrees with its non-hydrogen-bonded state and a compression of the OH bond as the lattice contracts. The shortening is not resolved in the neutron study in which the O-H (O-D) bond-length is, within error, invariant (Welch and Marshall 2001).

Hydrogen bonding in clinocllore above 6 GPa

The linear pressure dependence of all OH-stretching frequencies together with the continuous, positive pressure shifts of the lattice modes of clinocllore to ~6 GPa show that no major structural changes occur in this pressure range, in the hydrogen- as well as metal-oxygen-sublattice. At higher pressures the mode behavior becomes more complicated, revealing considerable complexity of hydrogen bonding in clinocllore under high compression.

Near 9 GPa, beyond the pressure range where crystallographic data were obtained, a sharp discontinuity occurs in the pressure dependence of the interlayer OH modes reflecting strong changes in the OH-bonding environment. The very high vibrational frequencies at 9 GPa (>3725 cm⁻¹) together with their positive frequency shifts (~10 cm⁻¹GPa⁻¹) under further compression to 16 GPa are characteristic for (nearly) unbonded hydroxyl groups. Therefore, we interpret the 9 GPa discontinuity as a reorganization of the interlayer hydrogen bonding involving a transition to a very weakly hydrogen-bonded (including multi-furcated hydrogen-bonds) or non-hydrogen-bonded state. As the positive frequency shifts above 9 GPa are significant (10 cm⁻¹/GPa compared to ~1.5 cm⁻¹/GPa for the non-hydrogen bonded talc-like OH), not only a simple shortening of the OH bond length due to compression, but also additional effects such as cation repulsion are likely to determine the frequencies of these vibrations (Lutz 1995; Hofmeister et al. 1999).

The sharp ~9 GPa transition was also revealed in our high-pressure synchrotron X-ray diffraction study of the same sample (Welch et al., in preparation): only basal spacings show a dramatic discontinuity in the pressure dependence around 9 GPa, whereas *d*-spacings at high angles to (001), such as (060) and (33 $\bar{1}$), do not show discontinuous behavior. This implies that the discontinuity is primarily associated with a change in the interlayer topology, supporting the interpretation of the Raman data.

A possible trigger for the transition near 9 GPa might be that the approach of the basal tetrahedral O atoms toward the interlayer O atoms under compression gets to its limit. The pressure-induced amorphization of portlandite at 14 GPa (Kruger et al. 1989) has been correlated with the O²⁻-O²⁻ contact distance of ~2.7 Å (Nagai et al. 2000). If we use the bulk modulus of synthetic end-member clinocllore determined by Welch and Crichton (2002), $K_0 = 81.0 \pm 0.5$ GPa ($K'_0 = 4$), to calculate the pressure at which the O atom contact distance is reached in clinocllore, we obtain a "contact pressure" of ~9 GPa. A compression limit of the O_{basal 2:1}...O_{interlayer} space at 7–10 GPa is also indicated by the closure of the hydrogen-bond angle under compression: an angle of ~130°, the reported minimum for hydrogen-bond angles (Lutz 1995), would be reached in the clinocllore structure at pressures ≤9 GPa based on a linear extrapolation of the neutron data (Welch and Marshall 2001, their Fig. 8). As 9 GPa is the pressure at which we observe the jump in the interlayer OH mode frequencies, we propose that the change in the state of hydrogen bonding in clinocllore can be associated with the O²⁻-O²⁻ contact distance of 2.7 Å. Portlandite-like amorphization caused by pressure-induced frustration of the H sublattice (Raugei et al. 1999) is not a topological possibility for clinocllore because its OH dipole array

is very different from that of portlandite.

The discontinuity near 16 GPa involves the hydroxyl groups of the brucite-like layer as well as the hydroxyl groups of the 2:1 layer and is, therefore, likely to be associated with a change in the overall compression mechanism of the structure. The discontinuities in the pressure dependencies of the OH-stretching frequencies are also evident in the pressure dependence of the 679 cm^{-1} mode. This observation confirms that bands at 650–800 cm^{-1} contain a contribution from OH vibrations (Prieto et al. 1991). The 358 cm^{-1} mode is the only observed mode between 100 and 1100 cm^{-1} that is completely unaffected by the discontinuities of the OH vibrations, showing that the metal-oxygen sublattice, or at least parts of it, do not undergo drastic changes up to 26.5 GPa. It is unlikely that the observed transitions are due to breaking of Si-O, Al-O, or Mg-O bonds, because the transitions are completely reversible, without hysteresis, on decompression.

Positive pressure dependencies of OH-stretching frequencies are much less common than negative dependencies where pressure-enhanced hydrogen bonding is thought to involve shortening of the hydrogen bond and a concomitant lengthening of the hydroxyl bond. The causes of positive shifts are not well understood, in part because there is a dearth of experimental data relating to them. Recently, significant positive pressure-induced frequency shifts have been observed in humites (e.g., Liu et al. 1999; Lin et al. 2000). They were explained as being due to a combination of H-H repulsion and hydrogen-bond elongation toward an empty polyhedron. The positive shifts of the hydrogen-bonded hydroxyl groups observed for clinocllore are much higher than those in humites. Possible explanations for the observed dramatic changes in the OH-stretching region concomitant with unusually high OH frequencies include anion- and cation-repulsion [O-O, neighboring Si-H and (Mg,Al)-H] and pressure-induced changes in the hydrogen bond properties.

ACKNOWLEDGMENTS

Work supported in part by NERC grant GR3/10912 to APJ, NERC grant GR9/03560 to MDW, and an Oxford University Graduate Scholarship in Physical Sciences to AKK. We particularly thank K. Refson for discussions and the referees for constructive comments.

REFERENCES CITED

- Bailey, S.W. (1988) Hydrus Phyllosilicates. *Mineralogical Society of America, Reviews in Mineralogy*, 19, 347–398.
- Baker, J. and Holland, T.J.B. (1996) Experimental reversal of chlorite compositions in divariant $\text{MgO}+\text{Al}_2\text{O}_3+\text{SiO}_2+\text{H}_2\text{O}$ assemblages. *American Mineralogist*, 81, 676–684.
- Brown, B.E. and Bailey, S.W. (1962) Chlorite polytypism: I. Regular and semi-random one-layer structures. *American Mineralogist*, 47, 819–850.
- Hofmeister, A.M., Cynn, H., Burnley, P.C., and Meade, C. (1999) Vibrational spectra of dense, hydrous magnesium silicates at high pressure: Importance of the hydrogen bond angle. *American Mineralogist*, 84, 454–464.
- Jenkins, D.M. (1981) Experimental Phase Relations of Hydrous Peridotites Modelled in the System, $\text{H}_2\text{O}-\text{CaO}-\text{MgO}-\text{Al}_2\text{O}_3-\text{SiO}_2$. *Contributions to Mineralogy and Petrology*, 77, 166–176.
- Jenkins, D.M. and Chemosky, J.V. (1986) Phase equilibria and crystallochemical properties of Mg-chlorite. *American Mineralogist*, 71, 924–936.
- Jephcoat, A.P., Mao, H.K., and Bell, P.M. (1987) Operation of the Megabar Diamond-Anvil Cell. *Hydrothermal Experimental Techniques*, 19, 469–506, Wiley-Interscience.
- Kruger, M.B., Williams, Q., and Jeanloz, R. (1989) Vibrational spectra of $\text{Mg}(\text{OH})_2$ and $\text{Ca}(\text{OH})_2$ under pressure. *Journal of Chemical Physics*, 91, 5910–5915.
- Lin, C.C., Liu, L.G., and Mernagh, T.P. (2000) Raman spectroscopic study of hydroxyl-clinohumite at various pressures and temperatures. *Physics and Chemistry of Minerals*, 27, 320–331.
- Liu, L.G., Lin, C.C., and Mernagh, T.P. (1999) Raman spectra of norbergite at various pressures and temperatures. *European Journal of Mineralogy*, 11, 1011–1021.
- Lutz, H.D. (1995) Hydroxide Ions in Condensed Materials - Correlation of Spectroscopic and Structural Data. *Structure and Bonding*, 82, 86–103.
- Nagai, T., Ito, T., Hattori, T., and Yamanaka, T. (2000) Compression mechanism and amorphization of portlandite. $\text{Ca}(\text{OH})_2$: structural refinement under pressure. *Physics and Chemistry of Minerals*, 27, 462–466.
- Peacock, S.M. (1990) Fluid Processes in Subduction Zones. *Science*, 248, 329–337.
- Prieto, A.C., Dubessy, J., and Cathelineau, M., (1991) Structure-Composition Relationships in Trioctahedral Chlorites: A Vibrational Spectroscopic Study. *Clays and Clay Minerals*, 39, 5, 531–539.
- Raugei, S., Silvestrelli, P.L., and Parinello, M. (1999) Pressure-induced frustration and disorder in $\text{Mg}(\text{OH})_2$ and $\text{Ca}(\text{OH})_2$. *Physical Review Letters*, 83, 2222–2225.
- Serratos, J.M. and Viñas, J.M. (1964) Infra-red Investigation of OH Bonds in Chlorites. *Nature*, 202, 999.
- Shirozu, H. (1980) Cation distribution, sheet thickness, and O-OH space in trioctahedral chlorites—an X-ray and infrared study. *Mineralogical Journal*, 10, 14–34.
- Welch, M.D. and Crichton, W.A. (2002) Compressibility of clinocllore to 8 GPa at 298 K and a comparison with micas. *European Journal of Mineralogy*, 14, 561–565.
- Welch, M.D. and Marshall, W.G. (2001) High-pressure behavior of clinocllore. *American Mineralogist*, 86, 1380–1386.
- Welch, M.D., Barras, J., and Klinowski, J. (1995) A multinuclear NMR study of clinocllore. *American Mineralogist*, 80, 441–447.
- Xu, J. and Mao, H.K. (2000) Moissanite: A window for high-pressure experiments. *Science*, 290, 783–785.

MANUSCRIPT RECEIVED JUNE 26, 2002

MANUSCRIPT ACCEPTED OCTOBER 17, 2002

MANUSCRIPT HANDLED BY ALISON PAWLEY